Open access Journal **International Journal of Emerging Trends in Science and Technology**

Performance of Fixed Speed Wind Turbine Generating Systems in Power Flow Solutions

Authors
Pichuka Anvesh[1], G. Hari Krishna[2], Sk. Jan Bhasha[3]

[1]PG Student [EPS], Dept. of EEE, ASIT, Gudur, SPSR Nellore (D), Andhra Pradesh, India
Email: *pichukaanvesh@gmail.com*
[2]Assistant Professor, Dept. of EEE, ASIT, Gudur, SPSR Nellore (D), Andhra Pradesh, India
Email: *ghk1984@gmail.com*
[3]Associate Professor, Dept. of EEE, ASIT, Gudur, SPSR Nellore (D), Andhra Pradesh, India
Email: *janbhasha@gmail.com*

Abstract
An increased penetration of wind turbine generating systems into power grid calls for proper modeling of the systems and incorporating the model into various computational tools used in power system operation and planning studies. This paper proposes a simple method of incorporating the exact equivalent circuit of a fixed speed wind generator into conventional power flow program. The method simply adds two internal buses of the generator to include all parameters of the equivalent circuit. For a given wind speed, the active power injection into one of the internal buses is determined through wind turbine power curve supplied by the manufacturers. The internal buses of the model can be treated as a traditional P–Q bus and thus can easily be incorporated into any standard power flow program by simply augmenting the input data files and without modifying source codes of the program. Available Transfer Capacity (ATC) of the power system also observed without and with fixed speed wind generator. The effectiveness of the proposed method is well discussed with various cases on the IEEE 30-bussystem.
Keywords: *fixed speed wind turbine, P-Q bus, ATC*

INTRODUCTION

Wind is the fastest growing renewable energy technology in the world and is considered as the most cost effective way of generating electrical power from renewable sources. The principle of a wind turbine generating system (WTGS) is based on two wellknown processes: conversion of kinetic energy of moving air into mechanical energy, and conversion of mechanical energy into electrical energy. The integration of WTGS into power grid has increased significantly in recent years [1]. In fact, worldwide installation of wind turbines has increased from about 5 GW in 1995 to more than 275 GW in 2012 [2]. Increased penetration of wind generators into power grid calls for proper modeling of the WTGS and incorporating the model into various computational tools used for steady state and dynamic analyses of power systems. A WTGS can be classified into fixed speed, limited variable speed and variable speed [3,4]. The fixed speed (or Type-1) generating system employs a squirrel-cage induction generator (SCIG) which is directly connected to the grid through a step-up transformer. A soft starter and shunt capacitors are usually used for smoother connection and reactive power support. A SCIG operates within a very narrow speed range (around the synchronous speed) and that is why it is considered as a fixed speed generator. The limited variable speed (or Type-2) generating system employs a wound-rotor induction generator (WRIG). The speed of the generator can be varied within a certain range by adjusting external rotor impedance of the generator. The variable speed generating system requires either partial-size or full-size converters. The generating system with partial-size converters (or Type-3) employs a doubly feed

induction generator (DFIG). The rotor excitation of the DFIG is supplied by a current regulated voltage source converter, which adjusts the magnitude and phase angle of rotor current almost instantly. The rotor side converter is connected back-to-back to a grid side converter. The generating system with full-size converter (or Type-4) usually employs a permanent magnet synchronous generator (PMSG), which is connected to the grid through full size back-to-back voltage source converters or a diode rectifier and a voltage source converter. In terms of power control, a wind turbine (WT) can be classifiedinto stall-controlled and pitch-controlled [5,6]. A stall-controlled WT has a fixed blade angle but the blades are carefully designed to reduce aerodynamic efficiency at higher wind speeds to prevent the extraction of excessive power from the wind. On the other hand, a pitch-controlled WT adjusts the blade pitch angle to limit the power capture at higher wind speeds. Most of the earlier wind farms used fixed speed stall-controlled wind turbines [7]. A fixed speed WT is also known as ''Danish concept'' as it was developed and widely used in Danish wind farms. However, the present trend is to use variable speed WTs that employ DFIGs. In both cases, it isvery important to incorporate the model of WTGS into existing computational tools used in power system studies.

The steady state behavior of a power system is usually evaluated through power flow calculations which mainly determine the complex voltage (magnitude and phase angle) of all buses. The complex power flow through each branch and other quantities are then calculated using the complex bus voltages. In power flow calculations, the buses of a power system are classified into swing (or V-d) bus, voltage-controlled (or P-V) bus and load (or P–Q) bus [8,9]. For a P–V or a P–Q bus, the active power injection P into the bus is known or specified. Fortunately, most of the WT manufacturers provide the power curve (mechanical power verses wind speed) of the turbine [10,11]. By knowing wind speed, the corresponding turbine mechanical power can immediately be determined from the curve. In power flow analysis, a fixed speed wind generating system is usually represented by a P–Q model or an R-X model [12–16]. In P– Q model, the reactive power drawn by the generator is first approximated in terms of its active power and terminal voltage. The per-phase steady state equivalent circuit of the generator, with some approximations, is used for this purpose. For a given wind speed, the generator bus is treated as a P–Q bus with varying reactive power, in contrast to a conventional P–Q bus where it remains constant. This model may not provide correct results because of the approximations used in evaluating the reactive power. An accurate P–Q model of a SCIG is described in [16] but the model need to be evaluated as a part of the iterative process of the power flow program. A DFIG or a PMSG can also be represented by a P–Q model with varying reactive power as it is controlled by the converter. Such generators can also be operated either as constant power factor mode or constant voltage mode. In R-X model, a SCIG generator is represented by an equivalent impedance obtained from its steady state equivalent circuit [12,13]. In power flow analysis, the impedance is then considered as a shunt element at the generator terminal bus. However, the impedance of the generator is not constant but highly dependent on operating slip which is not known apriori. In [12], a sub-problem is formulated to calculate the slip iteratively. Alternatively, the jacobian of the power flow program can be modified to includethe slip [17]. In both cases, significant modifications to the source codes of the program are needed. This paper proposes a simple method of incorporating the exact equivalent circuit of a fixed speed wind generator into a power flow program that does not require any modification to source codes of the program. The ATC of the system is also observed based on the algorithm in [29] without and with wind generator. The proposed method is then tested and discussed well on the IEEE 30-bus systems.

2. Power flow method

Power flow is one of the most important computational tools used in power system operation and planning studies. It solves the active and reactive power equations to find bus voltage magnitudes and phase angles. The injected active

power (Pi) and reactive power (Qi) into bus i of an n-bus power system can be written as [8].

$$P_i = V_i^2 G_{ii} + V_i \sum_{j=1; \neq i}^{n} V_j \left(B_{ij} \sin \delta_{ij} + G_{ij} \cos \delta_{ij} \right) \quad (1)$$

$$Q_i = -V_i^2 B_{ii} + V_i \sum_{j=1; \neq i}^{n} V_j \left(G_{ij} \sin \delta_{ij} - B_{ij} \cos \delta_{ij} \right) \quad (2)$$

Here $Y = (G + jB)$ and $\delta ij = (\delta i - \delta j)$. Vi and Vj are the voltage magnitude of buses i and j, respectively. δi and δj are the voltage phase angle of buses i and j, respectively, and Y is the bus admittance matrix. The Newton Raphson (NR) method is commonly used to solve the above equations. The governing equation of the method can be written as

$$\begin{bmatrix} \Delta P \\ \Delta Q \end{bmatrix} = \begin{bmatrix} \frac{\partial P}{\partial \delta} & \frac{\partial P}{\partial V} \\ \frac{\partial Q}{\partial \delta} & \frac{\partial Q}{\partial V} \end{bmatrix} \begin{bmatrix} \Delta \delta \\ \Delta V \end{bmatrix} \equiv [J] \begin{bmatrix} \Delta \delta \\ \Delta V \end{bmatrix} \quad (3)$$

The size of the jacobian matrix J in (3) is (n_{PV} + $2n_{PQ}$) _ (n_{PV} + $2n_{PQ}$), where n_{PV} is the number of P-V buses and n_{PQ} is the number of P–Q buses in the system. The computational algorithm of the method is well described in literature [8,9]. For most of the well-behaved systems, the NR method usually converges in 3–6 iterations.

3. Wind power

The mechanical power captured by a wind turbine (PT) can be written as [18,19].

$$P_T = \frac{1}{2} \rho A V_w^3 C_p (\lambda, \beta) \quad (4)$$

Here ρ is the air density (kg/m^3), A is the turbine blade swept area (m2), Vw is the wind speed (m/s), and Cp is the performance coefficient of the turbine. Cp is a function of tip speed ratio k and bladepitch angle b, and it can be expressed as [19]

$$C_p (\lambda, \beta) = c_1 \left[\frac{c_2}{\lambda_i} - c_3 \beta - c_4 \beta^{c_5} - c_6 \right] e^{\frac{-c_7}{\lambda_i}} \quad (5)$$

Where $\lambda_i = \left[\frac{1}{\lambda + c_8 \beta} - \frac{c_9}{\beta^3 + 1} \right]^{-1}$ and $\lambda = \frac{R \omega_T}{V_w} = \frac{R a_g \omega_T}{V_w}$

Here ω_T and ω_r are the angular velocity (rad/s) of the turbine and the generator rotor, respectively. R is the turbine blade length (m) and a_g is the gear ratio. The value of various constants (c1–c9) can be

determined from manufacturer data. The above equations are very useful in designing control system of a WT to maximize its efficiency. However, the objective of this paper is to determine the power flow results of a wind integrated power system and the evaluation of control strategy of WT is beyond the scope of the paper.
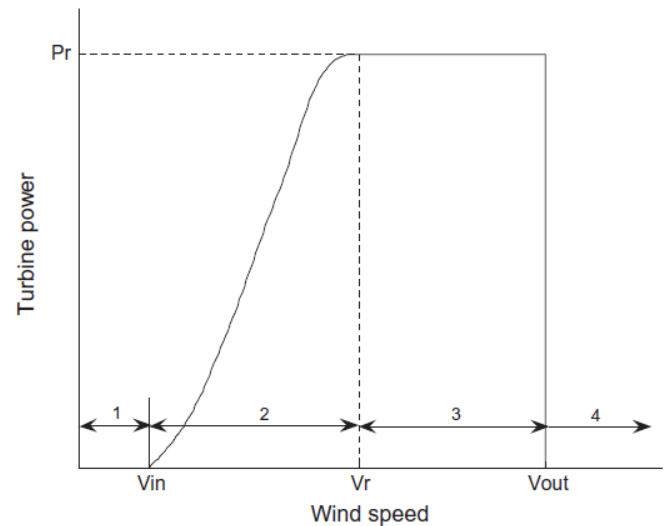

Fig. 1. Typical power curve of a wind turbine

A typical variation of turbine power against wind speed is shown in Fig. 1 where Vin, Vr and V out represent the cut-in wind speed, rated wind speed and cut-out wind speed, respectively, and Pr is the rated power of the turbine. It can be noticed in Fig. 1 that the turbine power is variable only in region 2 where the wind speed varies between Vin and Vr. In other regions (1, 3 and 4) or wind speeds, the turbine power is either zero or at rated value. Fortunately, most of the WT manufacturers provide the power curve and thus for a given wind speed, the turbine power can immediately be determined from the curve or a lookup table. In simulation studies, it is preferable to have piece-wise mathematical expressions of the power curve. Refs. [20,21] estimated the power in region 2 (Vin $\leq$Vw$\leq$Vr) through a quadratic function using the values of Vin, Vr and Pr. In this study, the turbine power PT in region 2 is expressed by the following polynomial

$$P_T = a_0 + a_1 V_w + a_2 V_w^2 + a_3 V_w^3 \quad (6)$$

The manufacturer data can be used to evaluate the coefficients a's of (6) using any standard curve

fitting technique. Fig. 2 shows acomparison of estimated power obtained through (6) with thecorresponding actual values of Vestas V100-1.8 MW wind turbinesupplied by the manufacturer [10]. The coefficients of (6) areobtained through 'polyfit' routine given in MATLAB using the manufacturerdata extracted at discrete wind speeds (at an interval of1 m/s) from cut-in wind speed of 3 m/s to rated wind speed of12 m/s.

Fig. 2 Comparison of estimated and actual turbine power, '—' estimated through (6); 'O' manufacturer supplied data.

Thus, mathematically, the turbine power P_T of Fig. 1 can beexpressed as

$$P_T = \begin{cases} 0; & V_w \leq V_{in} \\ (a_0 + a_1 V_w + a_2 V_w^2 + a_3 V_w^3); & if\ V_{in} \leq V_w \leq V_r \\ P_r; & V_r \leq V_w \leq V_{out} \\ 0; & V_w > V_{out} \end{cases}$$

(7)

A small fraction of turbine power is lost in the gearbox and theremaining power can be considered as input mechanical power Pmto the generator. Thus,

$P_m = \eta_g P_T$ (8)

Here η_g is the efficiency of the gear box. The generator convertsmechanical power P_m into electrical power and feeds into the grid.The objective of this study is to properly model the WTGS andincorporate the model into a conventional power flow program toevaluate the steady state results of the system.

4. Model of WTGS and its incorporation into power flow program

Consider that the SCIG of a fixed speed WTGS is connected tobus k of a general power system through a step-up transformeras shown in Fig. 3. An external shunt capacitor is also connectedto the generator terminal to supply reactive power. Note that aSCIG always absorbs reactive power and that can be compensatedby the external shunt capacitor. Alternatively, a static var compensator (SVC) or a static synchronous compensator (STATCOM) canbe used to support reactive power. By selecting appropriate sizeof shunt capacitors and/or SVC/STATCOM, the terminal voltage ofthe generator can be regulated.

Fig. 3. Schematic diagram of a fixed speed WTGS connected to a power systemthrough a transformer.

Fig. 4. Equivalent circuit of a fixed speed WTGS including the transformer andshunt capacitor.

Fig. 5. Single-line representation of Fig. 4

The equivalent circuit of the SCIG including the transformer andthe shunt capacitor is shown in Fig. 4 where R1, R2, X1, X2 and Xmrepresent the stator resistance, rotor resistance, stator leakagereactance, rotor leakage reactance and magnetizing reactance,

respectively, of the generator, and s is the slip. Rt + jXt and -jXc represent the impedance of the transformer and the shunt capacitor,respectively.The power of the rightmost resistance R2(1-s)/s of Fig. 4 representsthe input mechanical power Pm to the generator and is suppliedby the WT. Note that, for generator operation, slip s isnegative and thus the power absorbed by the resistance is alsonegative. By knowing wind speed Vw, Pm can be determinedthrough (7) and (8). The generator converts Pm into electricalpower and delivers a complex output power (Pe + jQe) at its terminal (see Fig. 4). The difference between Pm and Pe represents the losses in R1 and R2. Note that the generator draws reactive powerfrom the system and thus Qe is negative. In fact, -Qe is the sum of reactive power losses in X1, Xm and X2.The circuit of Fig. 4 is redrawn in Fig. 5 by explicitly showingtwo internal buses (m and r) of the generator in addition to the terminalbus t and the system bus k. Bus m represents the air–gap linewhere the magnetizing reactance Xm is connected and bus r representsa fictitious rotor internal bus where the WT supplies mechanicalpower Pm to the generator. In Fig. 5, the power supplied by theWT is represented as negated load of _Pm + j0. Most of the previousmethods [12–16] considered only the generator terminal bus t anddetermined the complex power (Pe + jQe) with some approximationsor through significant modifications of computational algorithmof the power flow program. However, the proposedmethod extends the generator model beyond the terminal bus toinclude all parameters of the exact equivalent circuit of the generator.It may be mentioned here that the core loss resistance of thegenerator can also be included in parallel with jXm at bus m.By looking into Fig. 5, one can easily recognize that it is simply aradial system consisting of four buses (k, t, m and r), three series elements (Rt + jXt, R1 + jX1 and R2 + jX2), two shunt elements (-jXcand jXm) and a load (_Pm + j0) at bus r. The usual values of generatorparameters (R1≤X1, R2≤X2, and higher value of Xm) and load at bus r would allow to find the power flow solutions of the systemusing any standard power flow program by carefully incorporatingthe parameters of Fig. 5 into input data files (bus data and line data) without modifying source codes of the program. Note that a similar model is also used in [22,23] to represent an inductionmotor load in determining system loadability through power flowcalculations.As mentioned, a power flow program mainly determines thevoltage magnitude and phase angle of all buses which are thenused to compute power flow of all branches and other quantities.The complex power flow through branch R1 + jX1 near bus t (asshown in Fig. 5) represents the complex power (Pe + jQe) supplied by the generator at its terminal. The results associated with theinternal buses (m and r) of Fig. 5 are not important and thus maybe ignored or suppressed in the output of the program.

5. Results and discussions

The model of a fixed speed WTGS and its incorporation into aconventional power flow program is vigorously tested on the IEEE 30-bus system.In the IEEE 30-bus system, a number of wind farms(WF) are added throughout the network. It is considered that eachwind farm consists of a number of identical Vestas wind turbine(V100-1.8-MW) and SCIG (1.8-MW, 575-V, 0.9-pf) sets. A briefdescription of wind farms used in this study is given in Table 1.The power curve of the WT is obtained from [10] and it has a cutin,rated and cut-out wind speed of 3, 12 and 25 m/s, respectively.Even though the curve is for a pitch-controlled variable speed turbinebut the same data is used in this study because of the lack ofactual data for a large size fixed speed turbine. Ref. [24] demonstratedthat the power curve of a pitch-controlled fixed speed WTis not significantly different than that of a variable speed WT.

Table 1 Summary of various wind farms used in the IEEE 30-bus system

Wind farm	Number of WT and SCIG sets	Capacity in MW/MVA
A	5	9/10
B	10	18/20
C	15	27/30

Thegear efficiency η_g of the turbine is arbitrarily assumed as 95%. Theparameters of the generator are considered as R1 = 0.004843 pu,X1 = 0.1248 pu, R2 = 0.004377 pu, X2 = 0.1791 pu, and Xm = 6.77 pu. The leakage reactance of the step-up transformer is assumed as0.05 pu. The power flow results of the above three systems are obtainedby the NR method. The NR power flow program given in Power Toolbox [9] as well as developed in [25] is used for this purposeand both programs provide the same results.

The single line diagram and data of the IEEE 30-bus system are given in [9]. The system is modified by adding three wind farms A,B and C (as described in Table 1) at buses 14, 26 and 30, respectively.The network of the system is then augmented to includethe model of the wind farms. In the augmented network, the generatorterminal bus (bus t in Fig. 5) of wind farms A, B and C is numberedas 31, 34 and 37, respectively. The wind speed of wind farmsA, B and C is arbitrarily assumed as 12, 10 and 8 m/s, respectively.

The following are the cases are studies in this paper

1. Original system (without wind farms).
2. Modified system without shunt capacitor
3. Modified system with shunt capacitor
4. Modified system at higher wind speeds without shunt capacitor
5. Modified system at higher wind speeds with shunt capacitor

The power flow of the augmented network is then evaluatedwithout and with shunt capacitors. The MVAr rating of shunt capacitors is considered as 25% of respective wind farm capacityin MVA. The power flow of the system is also evaluated at higher wind speeds (Vr<Vw<Vout) to operate the wind farms at their rated capacity. In all cases, the NR method successfully converged in 4–5 iterations. Table 2 shows a comparison of voltage at system buses 14, 26 and 30 as well as generator terminal buses 31, 34 and 37. The voltage of buses 14, 26 and 30 in the original system (without wind farms) is also shown in the Table for comparison purpose. It can be noticed in Table 2 that the wind farms (without having shunt capacitors) slightly reduce the bus voltage because of drawing reactive power.

However, the voltage profile is improved when the shunt capacitors are added. At higher wind speeds (with shunt capacitors), the voltage profile again decreases because of drawing more reactive power.

Table 2 Comparison of voltage in per unit at some buses and real power losses (RPL) in MW of the IEEE 30-bus system.

Bus No	Case 1	Modified System with 3 Wind Farms			
		Case 2	Case 3	Case 4	Case 5
14	1.0429	1.0393	1.0484	1.0385	1.0479
26	1.0025	0.9817	1.0456	0.9726	1.0412
30	0.9953	0.9620	1.0360	0.9566	1.0330
31	-	1.0374	1.0477	1.0366	1.0472
34	-	0.9777	1.0445	0.9677	1.0395
37	-	0.9576	1.0360	0.9522	1.0330
RPL	17.528	14.421	13.487	14.660	13.550

Table 3 Comparison of ATC in MW of the IEEE 30-bus system

Seller/ Buyer	Case 1	Modified System with 3 Wind Farms			
		Case 2	Case 3	Case 4	Case 5
8/25	21.9	30.7	27.9	32.5	29.6
5/30	14.0	24.8	29.8	23.2	29.8
11/26	11.9	25.8	27.2	20.7	28.7
2/28	13.1	33.8	33.2	34.6	34.1

The real power system losses are also shown in in the Table 2. It has been observed that the loss reduction is higher when shunt capacitor existing. Table 3 shown the ATC values for the different cases and it has observed the ATC improved in all the cases.
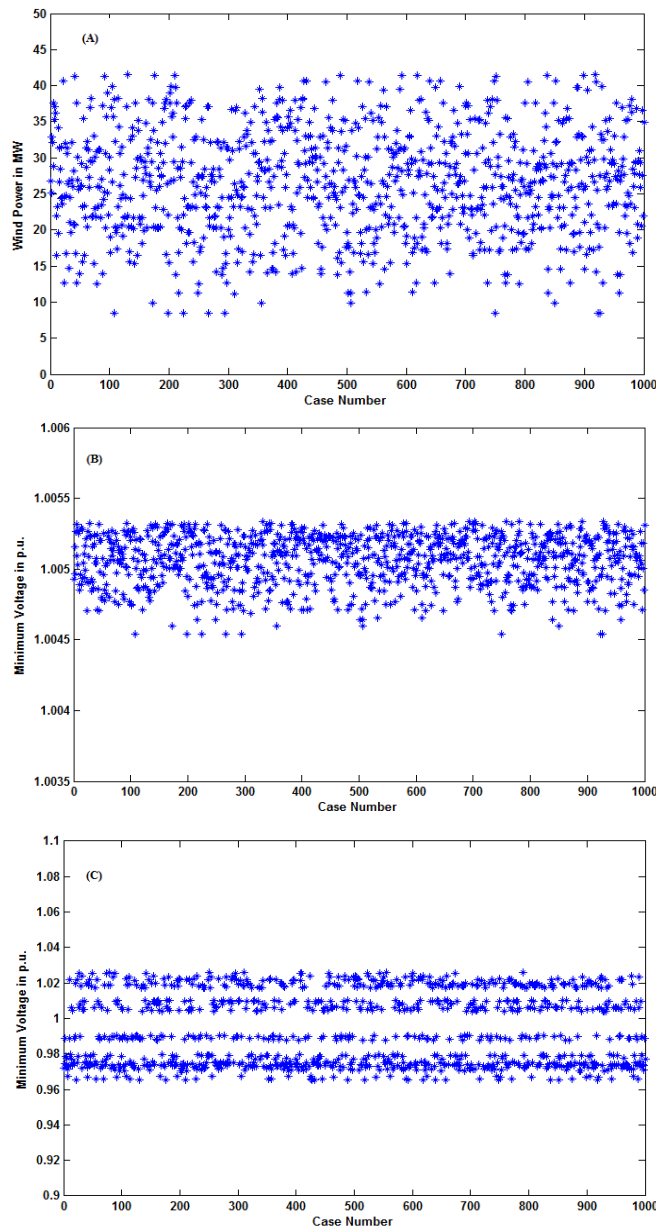
Fig. 3. Distribution of results of the 118-bus system for 1000 random cases of wind speeds: (A) wind power, (B) minimum voltage of buses 1–30, (C) minimumvoltage in the augmented network.

Finally, the wind speed of all wind farms is randomly selected through Weibull probability density function with a shape parameter of 2 and scale parameter of 9.027 (that corresponds to an average wind speed of 8 m/s [28]) using 'random' routine given in Matlab. The power flow problem of the modified network with shunt capacitors is then repeatedly solved for 1000 random cases of wind speeds. In all cases, the NR method successfully converged within 5 iterations. The distribution of total injected wind power (at internal bus r) is shown in Fig. 3(A). The minimum and the maximum power for 1000 random cases are found as 8.52 MW and

41.48 MW, respectively. Note that the total capacity of 3 wind farms is 54 MW. The distribution of minimum bus voltage of the original network (buses 1–30) is shown in Fig. 10(B) and it indicates that the minimum voltage varies within a very narrow range (1.0045pu – 1.0053pu) possibly because of low degree of penetration of wind power (<10%). However, the minimum voltage in the augmented network including the generator terminal and internal buses has a wider range (0.9655pu – 1.0258pu) as can be seen in Fig. 10(C). In all cases, the lowest voltage occurred at generator internal buses and which is not so important.

6. Conclusions

A simple method of incorporating the exact equivalent circuit of a fixed speed wind generating system into a conventional power flow program has been presented in this paper. The method simply augmented the network by adding two internal buses for each generating system. The new buses have the same property as a P–Q bus and thus can easily be incorporated into any power flow program without modifying the source codes of the program. However, augmentation of input data files of the program is needed to include the model or parameters of the generating system. The effectiveness of the proposed method is well discussed with IEEE 30-bus system. The power flow results of the simple system were also compared with the corresponding steady state values of dynamic responses of the system and are found to be in excellent agreement. It is also found that the incorporation of wind generators does not affect the convergence pattern of the power flow program. ATC also discussed and observed the maximum power flow between the seller and buyer.

References
1. Smith JC, Parsons B. Wind integration – much has changed in two years. IEEE Power Energy Mag 2011;9(6):18–25.
2. <http://www.thewindpower.net/index.php>.
3. Li H, Chen Z. Overview of different wind generator systems and their comparisons. IET Renew Power Gener 2008;2(2):123–38.

4. IEEE PES Wind Plant Collector System Design Working Group. Characteristics of wind turbine generators for wind power plants. In: Proc. 2009 IEEE power and energy society general meeting, Calgary, Canada, July 2009.

5. Muljadi E, Butterfield CP. Pitch-controlled variable-speed wind turbine generation. NREL, Report No. NREL/CP-500-27143, 2000.

6. Slootweg JG, Polinder H, Kling WL. Representing wind turbine electrical generating systems in fundamental frequency simulations. IEEE Trans Energy Conversion 2003;18(4):516–24.

7. Hansen AD, Hansen LH. Wind turbine concept market penetration over 10 years (1995–2005). Wind Energy 2007;10:81–97.

8. Kundur P. Power system stability and control. McGraw-Hill; 1993.

9. Saddat H. Power system analysis. McGraw-Hill; 1999.

10. <http://www.vestas.com/en/media/brochures.aspx>.

11. <http://www.energy.siemens.com/mx/en/power-generation/renewables/ wind-power/ wind-turbines/>.

12. Feijoo AE, Cidras J. Modeling of wind farms in the load flow analysis. IEEE Trans Power Syst 2000;15(1):110–5.

13. Eminoglu U. Modelling and application of wind turbine generating systems (WTGS) to distribution systems. Renew Energy 2009;34:2474–83.

14. Divya KC, Rao PSN. Models for wind turbine generating systems and their application in load flow studies. Electric Power Syst Res 2006;76: 844–56.

15. Liu Y, Wang W, Xu L, Ni P, Wang L. Research on power flow algorithm for power system including wind farm. Proc Int Conf Electric Mach Syst 2008:2551–5.

16. Feijoo A. On PQ models for asynchronous wind turbines. IEEE Trans Power Syst 2009;24(4):1890–1.

17. Esquivel CRF, Hermandez JHT, Alcaraz GG, Torres FC. Discussion of modelling of wind farms in the load flow analysis. IEEE Trans Power Syst 2001;16(4):951.

18. Heier S. Grid integration of wind energy conversion systems. 2nd ed. John Wiley; 2006.

19. Ackermann T. Wind power in power systems. John Wiley; 2006.

20. Pallabazzer R. Evaluation of wind-generator potentiality. Sol Energy 1995;55(1):49–59.

21. Villanueva D, Pazos JL, Feijoo A. Probabilistic load flow including wind power generation. IEEE Trans Power Syst 2011;26(3):1659–67.

22. Martins N, Henriques RM, Barbosa AA, Gomes S, Jr, Gomes CB, Martins ACB Impact of induction motor loads in system loadability margins and damping of inter-area modes. In: Proc. of the IEEE PES General Meeting, vol. 2, 2003. p. 1379–84.

23. Henriques R, Martins N, Ferraz JCR, Martins ACB, Pinto HJPC, Carneiro S, Jr. Impact of induction motor loads into voltage stability margins of large systems. In: Proc. of power systems computations conference, Seville, Spain, 2002.

24. Burton T, Jenkins N, Sharpe D, Bossanyi E. Wind energy handbook. 2nd ed. John Wiley; 2011.

25. Haque MH. Novel decoupled load flow method. IEE Proc C 1993;140(3):199–205.

26. Sim Power Systems User's Guide, Math Works, 2012.

27. Haque MH, Rahim AHMA. Determination of first swing stability limit of a multi machine power systems. IEE Proc C 1989;136 (6):373–9.

28. Masters GM. Renewable and efficient electric power systems. Wiley Interscience; 2004

29. Nireekshana T, KesavaRao G, Sivanagaraju S. Enhancement of ATC with FACTS devices using Real coded genetic algorithm. International Journal of Electrical Power and Energy Systems 2012:43:1276-1284

Authors Profile

Pichuka Anvesh was born in Andhra Pradesh, India. He received the B.Tech degree in Electrical and Electronics Engineering from JNTU, Anantapur in 2012 and pursuing M.Tech degree in Power Systems from ASIT, Gudur, JTNU, Anantapur, Andhra Pradesh, India. His areas of interest in the field of power systems, NON- Renewable energy sources and smart grid.

Mr .G. Hari Krishna was born in Andhra Pradesh, India. He received the B.Tech degree in Electrical and Electronics Engineering from kuppam Engineering College, Kuppam, A.P., in 2007. After the completion of M.Tech degree in Power Electronics from JNTU Anantapurin 2012, presently he is working as Asst. Professor Dept.EEE, Audisankara Institute of Technology- Gudur, Nellore, Andhrapradesh, India.

Mr. Jan Bhasha Shaik was born in Andhra Pradesh, India. He received the B.Tech degree in Electrical and Electronics Engineering from JNT University, Hyderabad in 2004 and M.Tech degree in Power & IndustrialDrives from JNT University Kakinada in2010. He is currently pursuing the Ph.D.degree at the JNT University, Anantapur, Andhra Pradesh, India. He had worked as an Assistant Professor and IEEE student Branch counsellor at Hi-Tech College ofEngineering, and worked as an Assistant professor at KL University Guntur, AP. Currently He is working as an Associate Professor at Audisankara Institute of Technology, Gudur, AP. He was the academic projectcoordinator for Under-Graduate & Post Graduate students.His areas of interest are HVDC, FACTS & SMART GRID.